JOURNAL OF MAGNETIC RESONANCE **130,** 305–316 (1998)
ARTICLE NO. MN971344

Magic Angle-Oriented Sample Spinning (MAOSS): A New Approach toward Biomembrane Studies[1]

Clemens Glaubitz and Anthony Watts[2]

Biomembrane Structure Unit, University of Oxford, South Parks Road, Oxford OX1 3QU, Great Britain

E-mail: glaubitz@bioch.ox.ac.uk, awatts@bioch.ox.ac.uk

Received June 26, 1997; revised December 4, 1997

The application of magic angle sample spinning (MAS) NMR to uniformly aligned biomembrane samples is demonstrated as a new general approach toward structural studies of membrane proteins, peptides, and lipids. The spectral linewidth from a multilamellar lipid dispersion is dominated, in the case of protons, by the dipolar coupling. For low-γ or dilute spins, however, the chemical shift anisotropy dominates the spectral linewidth, which is reduced by the two-dimensional order in a uniformly aligned lipid membrane. The remaining line broadening, which is due to orientational defects ("mosaic spread") can be easily removed at low spinning speeds. This orientational order in the sample also allows the anisotropic intermolecular motions of membrane components (such as rotational diffusion, $\tau_c = 10^{-10}$ s) for averaging dipolar interactions to be utilized, e.g., by placing the membrane normal parallel to the rotor axis. The dramatic resolution improvement for protons which are achieved in a lipid sample at only 220 Hz spinning speed in a 9.4 T field is slightly better than any data published to date using ultra-high fields (up to 17.6 T) and high-speed spinning (14 kHz). Additionally, the analysis of spinning sidebands provides valuable orientational information. We present the first ^{1}H, ^{31}P, and ^{13}C MAS spectra of uniformly aligned dimyristoylphosphatidylcholine (DMPC) bilayers. Also, ^{1}H resolution enhancement for the aromatic region of the M13 coat protein reconstituted into DMPC bilayers is presented. This new method combines the high resolution usually achieved by MAS with the advantages of orientational constraints obtained by working with macroscopically oriented samples. We describe the general potential and possible perspectives of this technique.

Key Words: **solid-state NMR; MAS; oriented membranes; peptides, lipids.**

INTRODUCTION

Structural studies of biomembranes, especially membrane-bound proteins and peptides, by solid-state NMR, have undergone a remarkable development in recent years (*1*). The different approaches involve, on the one hand, static NMR on uniformly aligned samples (*2*) and, on the other, magic angle sample spinning (MAS) NMR applied to powder-type samples, as recently reviewed by Smith and Groesbeek (*3*). The clear potential of the first method is in acquiring molecular orientation as well as structure constraints. A remarkable resolution can be achieved in cases where the sample is extremely well oriented, as recently shown for the fd coat protein (*4*). The second approach has less requirements toward sample preparation, but allows rather specific studies such as intermolecular torsion angle and distance measurements or probing of specific interactions (*3, 5, 6*).

Specifically in the case of membrane-bound peptides, the two central questions to be resolved are the structure in the membrane and the orientation with respect to the membrane (*2*). The central technical difficulties are to obtain a sufficiently high resolution for the nuclei of interest (^{1}H, ^{13}C, ^{15}N), to utilize dipolar and J couplings for obtaining structural constraints, and to obtain information about the orientation of specific sites in the peptide with respect to the bilayer (*7*).

Here, the application of MAS to uniformly aligned membranes and for obtaining both orientation and structure information in one unified approach is demonstrated.

In order to explain the approach we start from the MAS point of view and summarize very briefly the theoretical foundations. The spin interaction Hamiltonian in spherical tensor notation (spin parameters A_{kq}, lattice parameters T_{kq}) is given by (*8*)

$$H = \sum_{k=0}^{2} \sum_{q=-k}^{+k} (-1)^q A_{kq}(t) T_{k-q}(t'). \qquad [1]$$

The time dependence of $A_{kq}(t)$ is due to sample spinning while $T_{kq}(t')$ arises from the spin precision in B_0. By neglecting nonsecular terms Eq. [1] simplifies to

$$H_0 = A_{00}T_{00} + A_{10}(t)T_{10} + A_{20}(t)T_{20}. \qquad [2]$$

[1] This work was supported by BBSRC (43/B04750) and the EU (TMR Contract FMRX-CT96-0004). C. Glaubitz is the recipient of a C. Rhodes Scholarship.

[2] To whom correspondence should be addressed.

1090-7807/98 $25.00

$A_{00}T_{00}$ is invariant under rotation and $A_{10}(t)T_{10}$ can be neglected in the first order (*8*), so that only $A_{20}(t)$ needs to undergo a rotation transformation:

$$A_{20}(t) = \sum_{q=-2}^{+2} A_{2q} e^{-iq(\omega_r t+\phi_0)} d^{(2)}_{q,0}(\theta). \qquad [3]$$

The sample is rotated by an angle $(\omega_r t + \phi_0)$ about the spinning axis and it can be seen at this point already that sidebands will appear at ω_r, $2\omega_r$ beside the central resonance. In the case of a very large spinning rate ω_r, a time-independent Hamiltonian is obtained:

$$\bar{H}_0 = A_{00}T_{00} + 1/2(3\cos^2\theta - 1)A_{20}T_{20}. \qquad [4]$$

Anisotropic interactions such as homonuclear and heteronuclear couplings as well as the chemical shift anisotropy will vanish at the magic angle (54.7°). In a powder-type sample, a spinning speed exceeding these interactions is needed. Due to their strongly coupled network of spins, protons are normally not used in solid-state NMR. Their large dipolar couplings of about 36 kHz far exceed available MAS spinning speeds (~25 kHz) which would be necessary to obtain a sufficient averaging and hence resolution. However, utilizing protons for biological solid-state NMR is rather attractive since in solution NMR dipolar and *J* couplings of protons deliver mainly the structural information which is normally obtained from selective labeling with low-γ nuclei (^{13}C, ^{15}N) in solid-state NMR. Being able to achieve a sufficient ^{1}H resolution in biological membranes would then permit the application of well-developed solution-state NMR techniques. Additionally, the signal/noise problem which occurs by selective labeling in biological material, which cannot normally be provided in large quantities, would be overcome. The first ^{1}H MAS spectra of lipids were published by Oldfield and co-workers (*9–11*) and a number of attempts have been undertaken to improve the proton resolution in solid-state NMR of biomembranes (*12–17*), mainly by applying ultra-high magnetic fields or by ultra-fast MAS spinning, and it has been possible to resolve lipid and some peptide resonances. However, the resolution enhancement one would expect from high-field/high-speed MAS has so far not been achieved (*12*). Here, we present and discuss a new approach which might help to overcome these problems.

For dilute or low-γ nuclei (^{13}C, ^{15}N), however, only the chemical shift anisotropy dominates the broad lines in a static spectrum and this can be averaged by fast sample spinning in order to obtain a highly resolved spectrum. At the same time, applying high spinning speeds will usually cause all dipolar interactions (which are much weaker than ^{1}H–^{1}H couplings) to vanish. However, information about the strength of dipolar couplings between spins is needed for structural studies in biomembranes, and recoupling techniques such as rotational resonance (*18*), DRAMA (*19*), REDOR (*20*), MELODRAMA (*21*), or C7 (*22*) must be used to reintroduce the dipolar couplings back into the spectrum.

Consider now a sample which has a certain degree of orientational order, i.e., not a full powder. Only a residual line broadening in a static spectrum would be observed, which means that a much lower spinning speed would be sufficient to spin out the remaining orientational distribution in order to obtain a highly resolved spectrum which will be demonstrated below. If the sample spinning speed is smaller than the chemical shift anisotropy, spinning sidebands will appear, which is a well-studied phenomenon. Maricq and Waugh (*23*) pointed out the potential use of utilizing slow spinning MAS for obtaining chemical shift tensor information from the resolved spinning sideband structure. Herzfeld and Berger (*24*) suggested a graphical method and de Groot *et al.* (*25*) published an iterative numerical procedure for extracting chemical shift anisotropy and asymmetry parameters from sideband patterns. The intensity of the *N*th sideband in a sample which is transverse isotropic about the rotor axis is (*8, 23, 26*)

$$I_N(\sigma_{11}, \sigma_{22}, \sigma_{33}, \alpha, \beta) = |F_N|^2 \qquad [5]$$

with

$$F_N = \frac{1}{2\pi}\int_0^{2\pi} \times e^{i[-N\theta + C_1\sin\theta/\omega_r - S_1\cos\theta/\omega_r + C_2\sin 2\theta/2\omega_r - S_2\cos\theta/2\omega_r]}\, d\theta \qquad [6]$$

and

$$C_1 = \omega_0 \sin\theta\cos\theta\{-3\sin\beta\cos\beta(\sigma_{33} - \sigma_{iso}) + \sin\beta\cos\beta\cos 2\alpha(\sigma_{11} - \sigma_{22})\}$$

$$S_1 = -\omega_0 \sin\theta\cos\theta\{\sin\beta\sin 2\alpha(\sigma_{11} - \sigma_{22})\}$$

$$C_2 = \omega_0 \sin^2\theta\{3/4\sin^2\beta(\sigma_{33} - \sigma_{iso}) + 1/4(1 + \cos^2\beta)\cos 2\alpha(\sigma_{11} - \sigma_{22})\}$$

$$S_2 = -\omega_0 \sin^2\theta\{1/2\cos\beta\sin 2\alpha(\sigma_{11} - \sigma_{22})\}.$$

θ is the magic angle; σ_{11}, σ_{22}, and σ_{33} are the diagonal elements of the chemical shift tensor in its principal axis system (PAS); and σ_{iso} is the isotropic chemical shift. The Euler angles α, β, and γ describe the rotation from the principal axis system into the rotor-fixed coordinate system. These rotations are invariant to the angle γ in samples with transverse isotropy about the rotor axis, which results in positive, absorptive sidebands (*26*). The sideband intensity in a powder sample would depend only on the three diagonal chemical shift tensor elements. However, in partially or fully ordered systems a strong orientational dependence of the

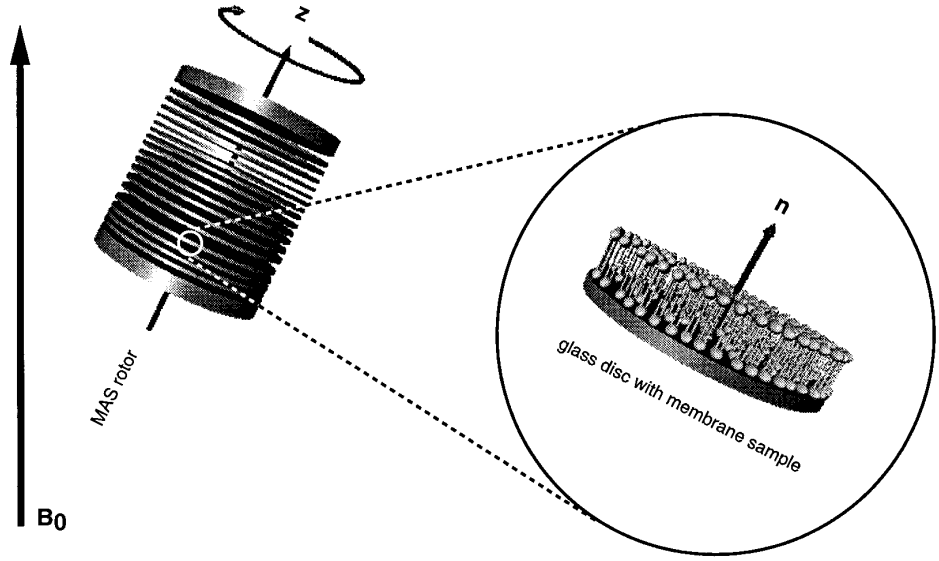

FIG. 1. Rotor design for MAOSS: A standard 7-mm Bruker MAS rotor contains a stack of thin glass plates with uniformly aligned phospholipid membranes. The membrane normal **n** is parallel to the rotor axis **z** which is tilted with respect to B_0 by the magic angle 54.7°.

sideband pattern can be observed and has potential use in determining tensor orientations, which has been demonstrated for the orientational distribution function in ordered polymers (*26*) and DNA fibers (*27*).

To exploit this information content in solid-state NMR studies on biomembranes, and to include the advantages of MAS on partially ordered systems in terms of spectral resolution, it is rather tempting to find a way to apply MAS to uniformly aligned membranes (magic angle-oriented sample spinning). As shown in Fig. 1, biomembranes can be uniformly aligned on thin glass disks (*28, 32*) which are mounted onto a MAS rotor, so that the membrane normal is parallel to the rotor axis. In this experimental setup, lipids would rotate about the magic angle ($\tau_c \sim 10^{-10}$ s), which would average the strong dipolar $^1H-^1H$ couplings, while additional sample rotation would average orientation defects. Both effects together allow a high ^1H resolution. Comparison between experiments in which the membrane normal is perpendicular to the rotor axis will be discussed below. The membrane-fixed coordinate system is identical to the rotor-fixed coordinate system. Spinning at various rates allows the sideband patterns to be analyzed as well as permits highly resolved spectra to be obtained at rather slow speeds (ω_r: 200–1000 Hz). In the experimental situation illustrated in Fig. 1, the membrane bilayer would be transverse isotropic; i.e., it has a macroscopic two-dimensional distribution about the rotor axis and each molecule in the membrane exhibits uniaxial symmetry. Considering a set of Euler angles $\{\alpha, \beta, \gamma\}$ needed to rotate the chemical shift tensor from its principal axis system into the rotor/membrane frame, β would be the only free angle and describes the tilt with respect to the membrane normal.

MATERIALS AND METHODS

Round, 0.01-mm-thin glass plates with a diameter of 5.4 mm (Marienfelde GmbH, Germany) were cleaned in nitric acid and methanol/ethanol and subsequently dried under a stream of nitrogen gas. The disk diameter was chosen to fit precisely into a standard Bruker 7-mm MAS rotor (RotoTec GmbH, Germany). The M13 coat protein was synthesized using standard solid-phase FMOC chemistry (NSR Centre, Nijmegen, The Netherlands); Asp was replaced with Asn. DMPC (dimyristoylphosphatidylcholine) was purchased from Sigma (UK) and used without further purification. To orient protein and lipids on the glass plates, protein and DMPC were codissolved in trifluoroacetic acid (Aldrich, UK) and chloroform (BDH) in a lipid to protein mole ratio of 15:1 and spread as one 10-μl drop onto the glass disks which were then thoroughly dried with a stream of nitrogen. Each drop contained 0.2 mg material and special care has been taken to ensure that the solvent covers the disk surface completely. After all material was added, samples were exposed to high vacuum for 12 h and hydrated by adding 0.25 μl D_2O (Aldrich) directly to each sample followed by an empty, clean disk on top. The same procedures were used for pure DMPC samples; however, no TFA was added. The prepared sample ''sandwiches'' were allowed to equilibrate in a hydration chamber for 48 h at 93% relative humidity (oversaturated KNO_3/D_2O solution) and 310 K. Glass plates (25) were placed on top of each other and mounted carefully onto a 7-mm MAS rotor using a specifically designed tool. Special KelF inserts on top and bottom guaranteed a fixed and stable position of each disk. The same samples were used for experiments with the membrane normal perpendicular to the rotor axis, but a different KelF insert held 8 disks in the

position needed. An amount of 5 μl D_2O was added to the rotor before closing it with a standard nonventing KelF cap.

For comparison with random distributions, multilamellar dispersion of M13 in its α-oligomeric form was prepared by reconstitution into DMPC as described previously (*29*).

All spectra were recorded at 100.63 MHz for ^{13}C, 160.3 MHz for ^{31}P, and 400.13 MHz for ^{1}H using a Bruker MSL 400 and double-resonance 7- and 4-mm MAS probes (Bruker, Germany). Typical pulse lengths were 6 μs. All ^{13}C and ^{31}P spectra were obtained with standard one-pulse experiments and 50 kHz proton decoupling. The spinning speed was controlled within a range of ± 3 Hz. An oscilloscope was used to control the rotor stability at low spinning rates. Static phosphorus NMR suggests a mosaic spread of $\pm 3°$ for the lipids in the sample.

The stability of sample orientation under spinning conditions was checked after each spinning experiment by comparison of static ^{1}H and ^{31}P spectra. Even after some hours of spinning, no line broadening could be observed which gives rise to the assumption that the lipid/protein samples are stably aligned on the glass disks in the rotor. The centrifugal acceleration at a spinning speed of 5000 Hz which applies to a single lipid or peptide located at the disk edge is 27,000g which is considerably smaller than the acceleration applied to membranes in ultracentrifugation. The bulk area compressibility modulus for a bilayer thickness of $d_t = 4$ nm is $K_A/d_t = |3 \times 10^{-7}|$ N/m^2 (*30*). This means that a single lipid of 2 nm length and 0.5 nm^2 cross-sectional area experiences a lateral force of $|5 \times 10^{-11}|$ N. This force is much larger than the centrifugal force at the disk edge at a spinning rate of 5000 Hz of $F_c = |3 \times 10^{-18}|$ N. All experiments described here were carried out at speeds not exceeding 3000 Hz.

Calculations of spinning sideband intensities were performed on an SGI INDY 4600 workstation using the program cc2 for simulation of homonuclear two-spin systems in the presence of magic angle spinning, written by Levitt (*31*).

RESULTS

^{1}H MAOSS: Resolution Enhancement

The static ^{1}H spectrum of a multilamellar dispersion of DMPC/D_2O in its fluid (Lα) phase at 318 K is shown in Fig. 2a. By uniformly aligning DMPC bilayers on glass disks with the membrane normal at the magic angle, as illustrated in Fig. 1, a dramatic linewidth reduction from about 20 to 6 ppm, which is just the chemical shift dispersion, is achieved (Fig. 2b). This effect has been illustrated previously by Smith *et al.* (*32*), where static ^{1}H spectra at the magic angle were used for estimating the amount of water in the samples. If one now starts spinning the sample, a dramatic spectral resolution is observed at a speed as slow as 220 Hz (Fig. 2c). This spectrum is plotted on an expanded horizontal scale from 6.0 to 0.0 ppm below Fig. 2c. A resonance assignment has been obtained from published literature (*9, 14*) and is given in Table 1 together with the full width at half-maximum for each relevant resonance. Spinning sidebands, which are not removed at this speed, are labeled with arrows in Fig. 2. The linewidth ranges from 29 Hz for the CH_2 resonance to only 9 Hz for the $N(CH_3)_3$ head group. This resolution is, to our knowledge, better than all published data so far using solid-state NMR techniques on biomembrane systems. The first reports of the application of MAS to biomembranes showed linewidths of 40 to 60 Hz at 11.7 T (*9, 10*). Some improvements have been made by ultra-fast spinning of up to $\omega_r = 14{,}000$ Hz, as shown by Davis *et al.* (*12*), where the linewidths were between 13 and 34 Hz (8.455 T). Pampel and Volke reported a linewidth of 20 Hz for the most narrow lines using an ultra-high field

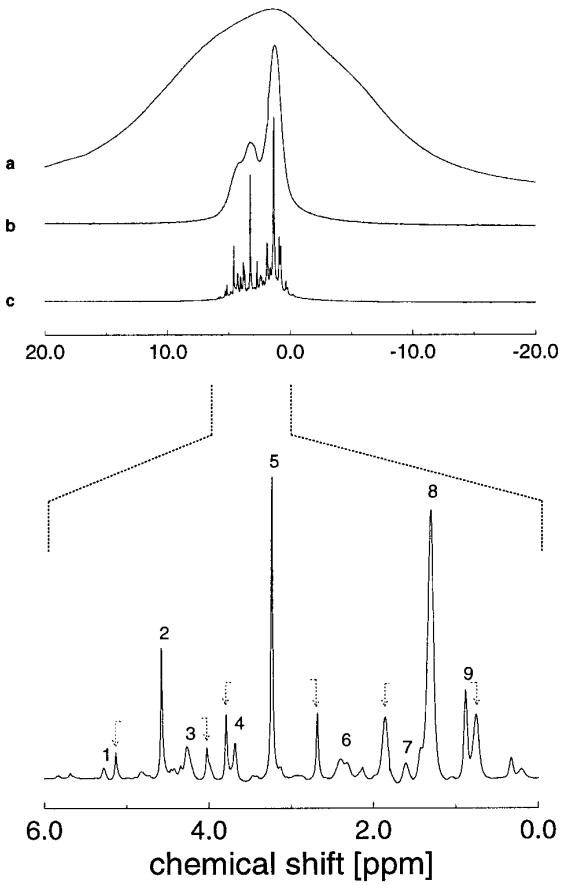

FIG. 2. 400.13-MHz proton spectra of uniformly aligned (b, c) and randomly distributed (a) DMPC in D_2O at the magic angle and at $T =$ 318 K. All resonances are already resolved at a spinning speed of 220 Hz. (a) Static, random distribution; (b) static, sample orientation as in Fig. 1; (c) same as (b) but at 220 Hz spinning speed. Spectrum (c) is shown below on an expanded horizontal scale (for resonance assignment and linewidth see Table 1). Sidebands are labeled by arrows. An exponential line broadening of 1 Hz was applied. 128 scans were acquired with a recycle delay of 2 s.

TABLE 1

Assignment of Proton Resonances for DMPC with Linewidth Obtained by Magic Angle-Oriented Sample Spinning (MAOSS) (Taken from Spectra in Fig. 2)

Peak	Group assignment	Linewidth $\Delta\nu_{1/2}$[Hz]
1	CH	16
2	HDO	9
3	α-CH_2	29
4	β-CH_2	20
5	γ-$N(CH_3)_3$	9
6	$CH_2\underline{CH_2}COO$	25/16
7	$\underline{CH_2}CH_2COO$	30
8	$(CH_2)_n$	29
9	CH_3	19

of 17.6 T and a spinning speed of 8000 Hz for their MAS studies (*15*).

The applicability of this method to membrane-bound peptides is illustrated in Fig. 3. The M13 coat protein, a 50mer membrane-bound peptide, has been reconstituted (see Materials and Methods) into DMPC in order to carry out standard MAS studies at 318 K and a spinning rate of ω_r = 10,000 Hz (Fig. 3a) and Fig. 3b is a vertical expansion of the aromatic region from 6.0 to 9.0 ppm of this spectrum. The signal arises from the amino acids Phe-11, Tyr-21, Tyr-24 and Trp-26, Phe-42, Phe-45. An oriented sample of M13 embedded in DMPC bilayers was prepared for MAOSS experiments. Figure 3c shows the expansion of the aromatic region obtained from an oriented sample at ω_r = 3000 Hz. The protein/lipid mole ratio in both cases was between 1:15 and 1:20. Some resonances can be resolved in the oriented sample (Fig. 3c), which can not be seen using high-speed MAS (Fig. 3b).

^{31}P: A ''Mechanical'' Example

The easiest example for demonstrating an orientation-dependent sideband pattern in oriented lipid membranes is shown in Fig. 4. Static ^{31}P spectra are compared with those obtained at a spinning speed of ω_r = 1000 Hz for a multilamellar dispersion of DMPC (Fig. 4a), and oriented DMPC samples with the membrane normal parallel (Fig. 4b) and perpendicular (Fig. 4c) to the rotor axis. The two different orientations were achieved by placing glass disks parallel and perpendicular to the symmetry axis of the MAS rotor. The isotropic line is labeled in each spectrum. The experiments were performed with the lipids in their fluid (Lα) phase. The static spectra of oriented samples suggest a mosaic spread of $\Delta\alpha = \pm 4°$ and the linewidth in these spectra is $\Delta\nu_{1/2}$ = 3 ppm, while isotropic line and spinning sidebands of the corresponding MAS spectra are narrowed to 1 ppm. The differences in the signal/noise between multilamellar dispersion and oriented samples is due to the fact that only five glass disks, each carrying 0.1 mg material, were used for these experiments. The sideband pattern changes dramatically by tilting the membrane normal mechanically from a parallel to perpendicular position with respect to the MAS rotor axis. The sideband pattern in Fig. 4a is the superposition of all possible orientations (''powder'').

^{13}C: A Molecular Example

Figure 5 illustrates the effect of orientation-dependent spinning sidebands for an example where the molecule itself is tilted with respect to the bilayer normal, and so to the rotor frame. It has been shown by a number of spectroscopic methods such as EPR or X-ray scattering that hydrocarbon chains in phospholipids, such as DMPC, are tilted from 0° to 30° with respect to the membrane normal while undergoing a phase transition from the liquid-crystalline to the gel phase (*58, 59*). This behavior is a good test case for demonstrating the applicability of the method to molecular orientation. Figures 5a and 5b show static spectra of oriented DMPC in the Lα (318 K) and Lβ phase (280 K). The corresponding spectra at a spinning rate of ω_r = 1080 Hz is plotted on top of these spectra, horizontally expanded from 12 to 65 ppm in Fig. 5c and Fig. 5d. A peak assignment is given in the figure legend (obtained from (*60*)). The intensity of the methylene resonance (C_4–C_{11}) decreases while undergoing the phase transition and two strong sideband intensities (+1, −1) appear. Since the entire chain is tilted, all resonances are affected, which is the reason that the C_2, C_3, C_{12}, and C_{13} resonances lose intensity and their sidebands become too weak to be detected. The linewidth for the MAS resonance lines increases with the phase transition from 1.1 ppm in Lα to 1.3 ppm in Lβ and the methylene resonance (C_4–C_{11}) is shifted by 2 ppm downfield. Computer simulations (see below) overlay Fig. 5c and Fig. 5d.

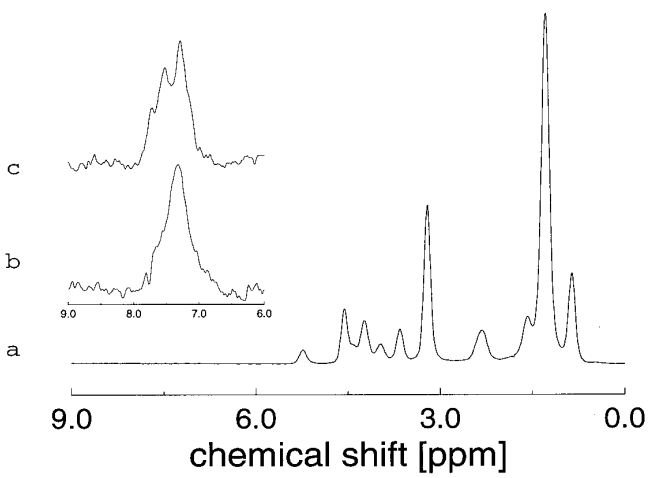

FIG. 3. ^{1}H MAS spectrum of a ''powder-type'' sample of DMPC containing M13 coat protein under conditions similar to those for Fig. 2 but at a spinning rate of 10,000 Hz (a). The inset shows a comparison of the aromatic region of M13 obtained under high-speed MAS conditions (b) and with oriented sample spinning (c). An exponential line broadening of 10 Hz was applied. 5000 scans were acquired with a recycle delay of 2 s.

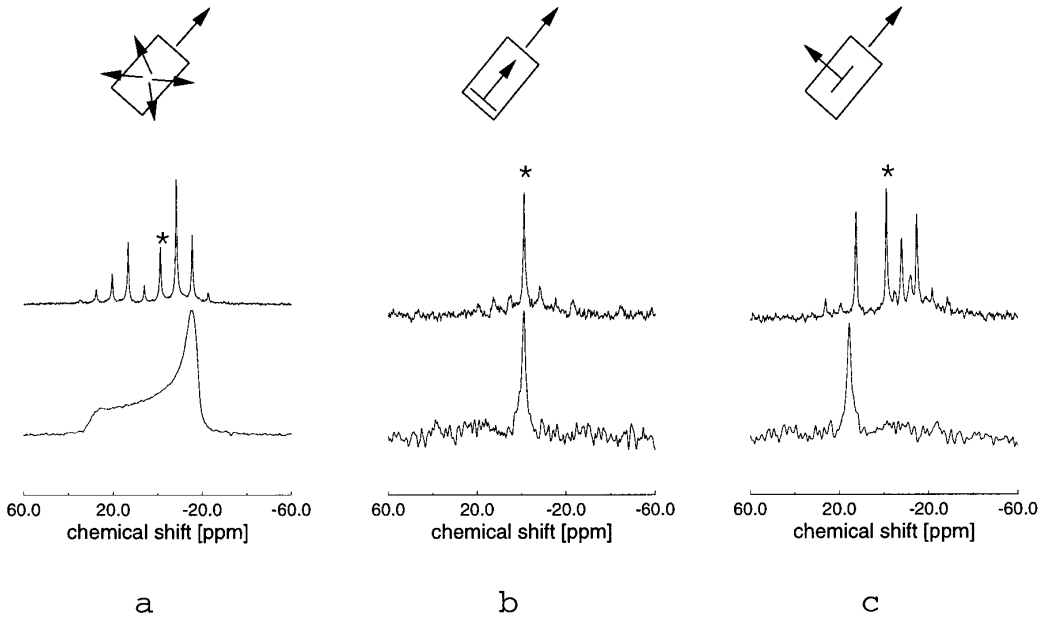

FIG. 4. ^{31}P spectra of DMPC at 318 K with different orientational distributions. All MAS spectra were recorded at ω_r = 1000 Hz. Static and MAS spectra of DMPC with a random orientational distribution (''powder'') (a) and static and MAS spectra of DMPC with the membrane normal parallel (b) and perpendicular (c) to the rotor axis. 2048 scans were acquired with a recycle delay of 2 s. The chemical shift is scaled with respect to phosphoric acid.

DISCUSSION

^{1}H Resolution

In order to understand the considerable ^{1}H resolution enhancement observed in MAOSS experiments, we must consider the special dynamic situation in lipid membranes, as well as the macroscopical sample geometry as illustrated in Fig. 1. The secular dipolar Hamiltonian, as discussed by Davis *et al.* (*12*), can be written as

$$H_D = -\frac{\gamma_{1H}^2\hbar}{2r_{12}^3}(3\cos^2(\beta_{PL}) - 1) \times [3I_{1Z}I_{2Z} - \mathbf{I}_1\mathbf{I}_2], \quad [7]$$

where β_{PL} denotes the Euler angle (*33*) needed to rotate the dipolar tensor from the principal axis system into the laboratory frame (α_{PL} can be set to zero due to the symmetry of the dipolar tensor and γ_{PL} can be neglected in the secular part of the Hamiltonian). Dipolar interactions would vanish at the magic angle of β_{PL} = 54.7°. In lipid membranes, three motional modes can be found (*39*): internal motions (*trans–gauche* isomerization, $\tau_j \sim 10^{-11}$ s), intermolecular motions (rotational diffusion about long axis $\tau_{R\parallel} \sim 10^{-10}$ s, and ''wobbling'' of long axis $\tau_{R\perp} \sim 10^{-9}$ s), and collective motions where the entire membrane undergoes undulations (*40, 41*) ($10^{-3}\cdots10^{-6}$ s). As suggested by Davis *et al.* (*12*), placing oriented membranes in their fluid phase with all local membrane normals at the magic angle would produce considerable ^{1}H resolution enhancement in biomembranes, since the membrane normal is the axis of symmetry of the highly anisotropic intermolecular motions, and all dipolar couplings would be projected onto this axis and therefore vanish. This situation is illustrated in Fig. 2b, where a dramatic line narrowing is achieved, but no lines can be resolved, which is probably why this approach was not pursued and more effort went into using ultrahigh speeds and high fields when exploiting protons for biomembrane studies (*12, 13, 15, 17*). However, the main cause of the residual line broadening in Fig. 2b is due to deviation from perfect uniform alignment. In a perfectly oriented membrane (mosaic spread $\Delta\alpha$ = 0°), every single lipid molecule would rotate with a long axis correlation time of 10^{-10} s about the magic angle. In this situation, no dipolar broadening would be expected. However, in the real experimental situation, it is impossible to prepare oriented membrane multilayers of this sufficiently high quality and low mosaic spread, with $\Delta\alpha$ = ±1°–3° being the best which can normally be achieved routinely (*32*). Using $\Delta\alpha$ and S_{HH}, the order parameter for the molecular segments under consideration, the Hamiltonian from Eq. [7] can be modified, taking mosaic spread and dynamics into account:

$$\langle H_D\rangle = -\frac{\gamma_{1H}^2\hbar}{2r_{12}^3}(3\cos^2(\beta_{PL} - \Delta\alpha) - 1) \times [3I_{1Z}I_{2Z} - \mathbf{I}_1\mathbf{I}_2]S_{HH}. \quad [8]$$

Due to the fast long axis molecular reorientation, all interac-

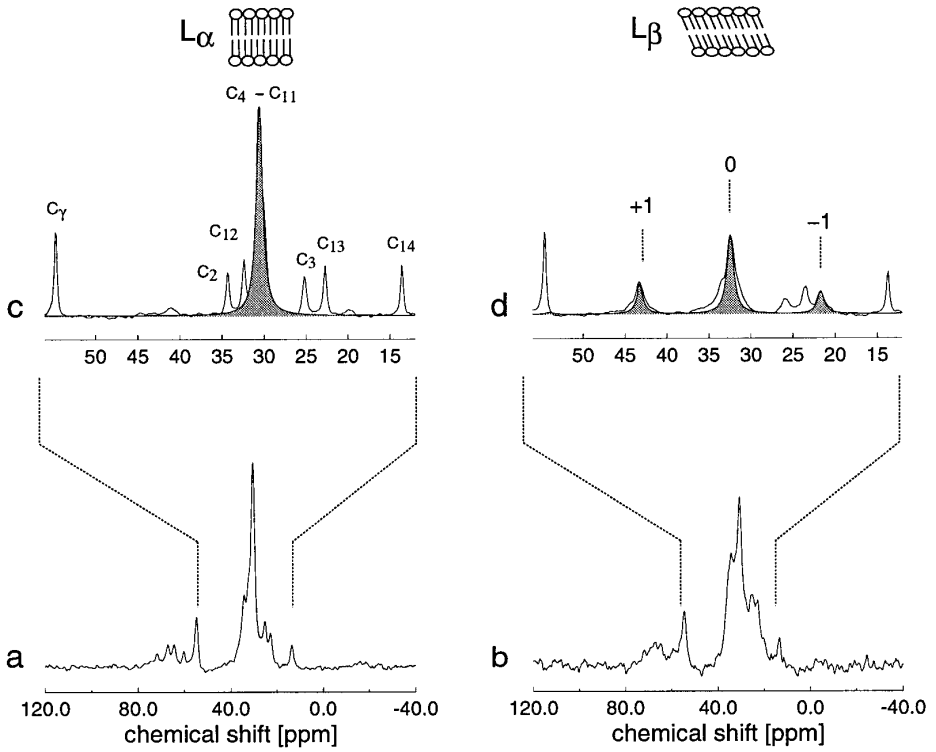

FIG. 5. ^{13}C spectra of uniformly aligned DMPC with the membrane normal parallel to the rotor axis. The acyl chains in DMPC are tilted from 0° to 30° while undergoing a phase transition from the Lα to the Lβ phase which is reflected in a change of the sideband pattern of the methylene group (C_4–C_{11} in spectrum (c)). (a) Static spectrum at T = 318 K (Lα), (b) static spectrum at T = 280 K (Lβ), (c) same as (a) but at ω_r = 1080 Hz, and (d) same as (b) but at ω_r = 1080 Hz. The shaded peaks are computer simulations for the two different orientations. Resonances C_2–C_{14} in spectrum (c) are from the fatty acyl chains and Cγ is from choline-Cγ in the polar head group (assignment from (*60*)). 4096 scans were acquired with a recycle delay of 2 s. The chemical shift is scaled with respect to TMS.

tions are scaled with the order parameter S_{HH} (*34, 35*). In estimating the contribution which nonperfect order would have on the linewidths in Fig. 2b, an average dipolar coupling of 36,000 Hz between adjacent protons, for example, in a methyl or methylene group is considered. The order parameter for chain methylene groups in lipids is $S_{HH^2}^{CH_2}$ = 0.25 and for methyl groups in the head group $S_{HH^3}^{CH_3}$ = 0.05; i.e., the dipolar coupling would be scaled down to 9000 and 1800 Hz, respectively. In the case of a perfect alignment of $\Delta\alpha = 0°$ these interactions would completely disappear, but with a mosaic spread of $\Delta\alpha = \pm 1°$, most lipids would actually not rotate exactly about but near the magic angle, and a residual dipolar coupling of up to 450 Hz for methylenes and 90 Hz for methyls would still cause a line broadening. However, this remaining dipolar coupling can easily be removed by slow macroscopic sample rotation about the magic angle, and explains the high resolution obtained at a rate of only 220 Hz (Fig. 2c). Since it is the dipolar coupling which mainly governs the linewidth in ^{1}H spectra, contributions from the chemical shift anisotropy are not widely studied, but Haeberlen and co-workers have determined chemical shift anisotropies of methylene protons to be 5–6 ppm (*36, 37*) which explains the appearance of sidebands in the spectrum of Fig. 2c.

The dynamics in lipid membranes is rather complex and covers time scales from 10^{-3} to 10^{-10} s (*38*). Here, we have demonstrated how to utilize rotational diffusion for resolution ^{1}H enhancement. In addition to dipolar coupling and chemical shift anisotropy, especially slow and intermediate time scale motions, in the frequency range of 10^{-3} to 10^{-6} s, in lipids were identified by Davis *et al.* (*12*) as another essential cause of line broadening. The contribution of an intermediate time scale motion with a correlation time τ_c to the linewidth of a MAS resonance at a speed of ω_r has been discussed by Maricq and Waugh (*23*) and can be estimated by (*12, 42*)

$$\frac{1}{T_2^{rot}} = \frac{\Delta M_2}{3\pi}\left(\frac{2\tau_c}{1 + (\omega_r\tau_c)^2} + \frac{\tau_c}{1 + 4(\omega_r\tau_c)^2}\right), \quad [9]$$

where ΔM_2 is the dipolar second moment being modulated by dynamic processes. These low-frequency fluctuations would cause additional line broadening. However, fluctuations in the orientation of the local bilayer normal, for example, in the form of undulations of the bilayer surface are mechanically suppressed in macroscopically oriented multilayers. The motional freedom along the bilayer normal

is restricted due to the solid support and due to the small interbilayer space caused by the absence of a large amount of free water.

The method presented here uses rotational diffusion (in the GHz range) for averaging dipolar couplings together with macroscopic sample spinning (~1 kHz) for averaging orientational defects while at the same time low-frequency dynamics (undulations), which would cause additional line broadening, are suppressed.

Even higher proton resolution can be achieved using MAOSS by applying higher fields and homonuclear decoupling techniques (*45*) and by improving the spinning and shimming properties of the MAS rotors. Shimming especially becomes critical in the experiment with a linewidth for γ-N$(CH_3)_3$ of 9 Hz where the best proton resolution which can be achieved with solvents with the MAS probe used here was 7 Hz. It has been discussed by Pampel and Volke (*15*) that the sample geometry is crucial for a narrow linewidth due to the shimming properties of MAS probes (*46*). Spinning speed instabilities can also cause additional line broadening.

To demonstrate the applicability to membrane-embedded proteins and peptides the 52 amino acid long M13 coat protein has been studied in a first attempt to apply MAOSS to larger systems. M13 has the primary sequence N-AEGDD PAKAA FNSLQ ASATE YIGYA WAMVV VIVGA TIGIK LFKKF TSKAS-C. It exists in the filamentous bacteriophage as a cytoplasmic protein, as a structural element, and as an integral membrane protein at different stages of the phage life cycle. Residues 21–39 form the hydrophobic core. M13 is an interesting test case, since it can be well oriented and is well characterized (*29, 47–50, 55*). Also, Opella and co-workers have carried out extensive and detailed multinuclear solution- and solid-state NMR on the coat protein of the very similar phage fd (*51–54*). M13 differs in only one residue from the fd coat protein. As described under Results, some spectral structures in the aromatic region can be resolved by MAS at 3000 Hz on oriented M13 samples which could not be resolved by spinning a multilamellar dispersion at 10,000 Hz (Fig. 3). However, M13 does not undergo rapid reorientations in a membrane (*54–57*), but, as in oriented lipid samples, slow motions are suppressed, which helps to achieve a resolution enhancement. Also, it has been shown that the side chains of aromatic residues are relatively flexible. Sykes and co-workers (*57*) studied M13 coat protein reconstituted into phospholipid vesicles and found by ^{19}F NMR that the aromatic rings in ^{19}F-labeled residues Tyr-21, Tyr-24, and Phe-11, Phe-42, and Phe-45 rotate freely about the C_β–Cγ bond by $\sim 4 \times 10^8$ s^{-1} while a ''wobbling'' about C_α–C_β with $\sim 2 \times 10^8$ s^{-1} is restricted within a range of 75°–90°. The high mobility determined is in good agreement with ^{1}H and ^{13}C studies of the aromatic residues of fd coat protein by Cross and Opella (*51*). These reorientations would project ^{1}H–^{1}H dipolar couplings onto the axis of symmetry and could finally be averaged by MAS. A similar case to the situation in oriented, fluid lipids would occur if the aromatic ring would rotate about the magic angle, which would require that the C_β–Cγ bond vector lie parallel to the membrane normal. However, the average orientation of this vector is not known. As discussed so far, the dynamic situation is not different from a multilamellar dispersion except that slow motions are suppressed. It is rather difficult and beyond the scope of this paper to assign any resonances in Fig. 3c to aromatic groups, because each group features a different and highly anisotropic motion which is reflected in the lineshape. There is also a strong pH dependency for the isotropic chemical shifts of these groups which could influence the lineshape in here (*51*). However, the fact that an improvement in resolution could be achieved underlines how slow motions can broaden ^{1}H MAS lines from biomembranes.

A much more favorable case would be the application of this method to peptides or protein fragments which undergo fast long axis reorientations. All points made about lipids would apply here and a good proton resolution is expected.

^{31}P: The ''Mechanical'' Example

Placing macroscopically ordered bilayers with the bilayer normal parallel and perpendicular to the MAS rotor axis demonstrates that in principle orientational information from spinning sideband patterns from fluid lipid membranes can be obtained. Having the membrane normal parallel to the rotor axis has a number of advantages over a perpendicular setup. A much better sample filling factor can be achieved by placing disks on top of each other into a round MAS rotor, and the mechanical spinning properties are easier to control in such a symmetrical sample alignment. The tilt angle could be determined from the chemical shift of the isotropic line in the static spectra of oriented samples, and this method is widely used in studies of lipid membranes (e.g., (*32, 61*)). However, the MAS approach described here has the advantage that it narrows lines and improves spectral sensitivity. Overlapping sideband patterns can easily be deconvoluted (*62*), as in a case where lines would overlap in the static spectra.

The most simple procedure for analyzing the information contained in these sideband patterns would be to calculate first the diagonal elements σ_{11}, σ_{22}, and σ_{33} of the chemical shift tensor in its principal axis system from a spectrum obtained for a multilamellar dispersion (Fig. 4a). With these data, Eq. [5] can be fitted to the sideband intensities obtained from oriented samples with β as the only free parameter. The error of this analysis is determined by the mosaic spread and the signal/noise ratio. More sophisticated methods have been developed and described and could be applied directly (*26, 63*).

^{13}C: The Molecular Example

The tilt of the lipid chains in the Lβ (gel) phase with respect to the bilayer normal is well established (*58*). Figure

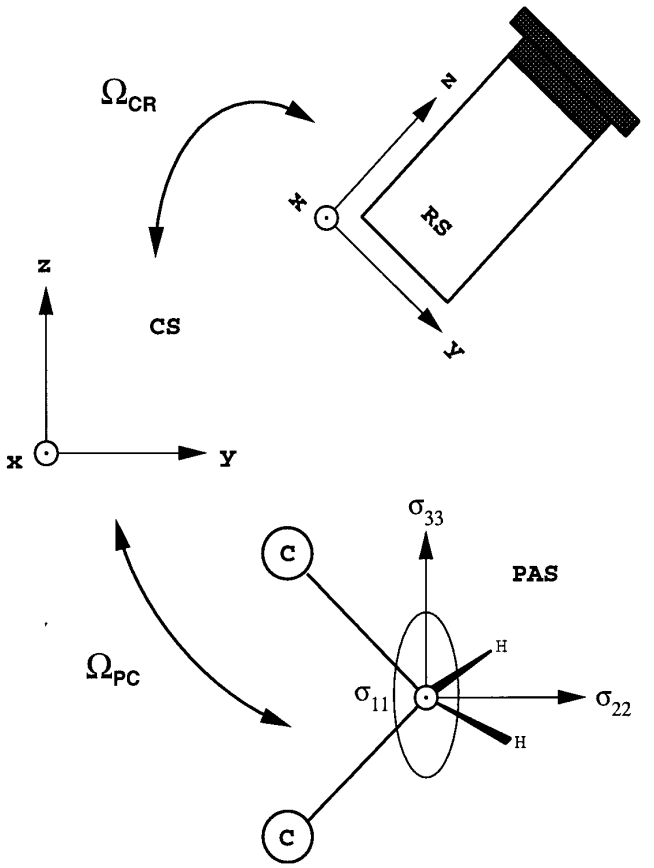

FIG. 6. Hierarchy of reference frames used for data analysis: The molecule-fixed coordinate system (CS) has been chosen to be identical with the principal axis system (PAS) for the chemical shift tensor of the methylenes C_4–C_{11} (Fig. 5c) with the *z* axis being the chain direction. A set of three Euler angles describes the transformation Ω_{CR} from CS into the rotor-fixed system RS which is identical with the membrane system.

5 shows a dramatic change in the ^{13}C MAOSS sideband pattern for the lipid when above and below the fluid Lα and gel Lβ phase transition. In order to be able to extract the chain tilt angle, the changes in the dynamic situation which would be reflected in a different chemical shift anisotropy need to be considered. The chemical shift anisotropy and asymmetry parameter from sideband intensities of low-speed spectra of multilamellar dispersions of DMPC in both phases (spectra not shown) have been determined for the Lα $\{\omega_{aniso} = 1000$ Hz, $\eta = 0.7\}$ and for the Lβ $\{\omega_{aniso} = 1750$ Hz, $\eta = 0.7\}$ phases. For the methylene ^{13}C chemical shift tensor from n-$C_{20}H_{42}$ crystals $\omega_{aniso} = 1800$ Hz and $\eta = 0.66$ have been found (*64*). The overall correlation time as determined by ^2H NMR by Weisz *et al.* (*39*) changes from $\tau_{\|} = 10^{-10}$ s for Lα to $\tau_{\|} = 10^{-7}$–10^{-6} s in Lβ, which explains the slight broadening of the MAS resonance lines (Eq. [9] applies here as well). Figure 6 defines the reference frames which are used to define the rotation of the ^{13}C chemical shift tensor (CST) of methylene into the rotor-fixed coordinate system. The principal axis system of the CST coincides with the vector joining both protons from the same CH_2 unit (**x**), the bisector of the H–C–H bond in the plane of these atoms (**y**), and the chain direction (**z**) (*64, 65*). Therefore, the set of Euler angles needed to perform a rotation from the PAS into the molecular reference frame CS is $\{\alpha_{PC} = 0, \beta_{PC} = 0, \gamma_{PC} = 0\}$. A second set of Euler angles relates CS to the rotor-fixed coordinate system RS which is identical with the bilayer system; that is, the membrane normal is parallel to the rotor axis. As discussed before, the bilayer exhibits transverse isotropy, since it is macroscopically and microscopically uniaxial. The only free angle is β_{CR} which describes the tilt of the chain to the membrane normal and for the spectral simulations averages over α_{CR} and γ_{CR} must be performed.

In order to make sure that the appearance of sidebands in Fig. 5d is not caused only by the increased chemical shift anisotropy, sideband intensities from low-speed spectra of multilamellar dispersions can be compared with those from oriented samples. In the gel phase, the intensity of sideband $+\mathbf{1}$ increases from 0.17 in the powder to 0.36 in the oriented system and $-\mathbf{1}$ increases from 0.09 to 0.18 (relative area intensities to the normalized isotropic line). In the fluid phase, however, intensities decrease slightly from 0.06 to 0.05 and 0.02 to 0.013 for $+\mathbf{1}$ and $-\mathbf{1}$ in powder and oriented system, respectively. These differences are due to the macroscopic order in the sample. Lineshape simulations have been performed for data both in Fig. 5c and in Fig. 5d and the best fits are shown over the experimental data. Figure 7 shows a series of calculations for the tilt angle $\beta_{CR} = 25° \cdots 35°$ in steps of 1° for a data set corresponding to the Lβ phase. At $\beta_{CR} = 0°$, sideband intensities would nearly vanish and the isotropic line only could be observed. Taking mosaic spread and signal/noise into account a molecular tilt of $\beta_{CR} = 33° \pm 6°$ is obtained, which is a reasonable result compared to the published tilt of 30° (*58*).

This experiment shows that the orientation of membrane components can be measured with the MAOSS method, and by applying sophisticated multidimensional sideband separation techniques, the orientational distribution functions of more complex systems such as peptides or proteins can be studied (*26*).

CONCLUSIONS

The applicability of MAS to uniformly aligned biomembranes using ^1H, ^{13}C, and ^{31}P (MAOSS) has been demonstrated. The advantage of this method over static NMR spectroscopy on oriented membranes is founded in the fact that deviations from perfect macroscopical orientation (''mosaic spread''), which would prevent well-resolved spectra, can be averaged by spinning at low speeds (<1 kHz). The orientational information which can be obtained from MAS on samples with a powder-type distribution is limited to relative orientations of tensors with respect to each other, for example, in the form of torsional and dihedral angles (*66–68*).

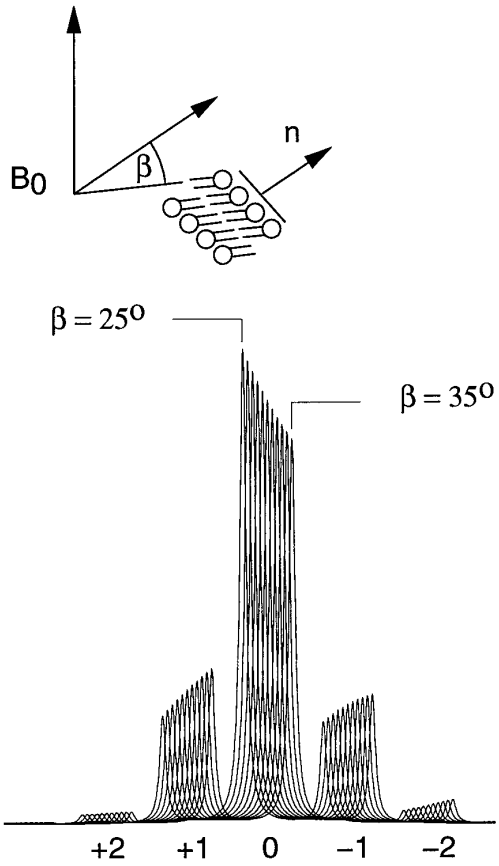

FIG. 7. Computer simulation as shown in Fig. 5d for a range of different tilt angles β from 25° to 35° in 1° steps. Sideband intensities vanish for $\beta = 0°$.

However, in this new approach, additional information about orientation with respect to the bilayer normal can be obtained from analyzing the spinning sideband patterns.

A further benefit is the different dynamic situation in macroscopically oriented membranes. By placing the sample with the membrane normal parallel to the rotor axis, molecular long axis rotations occur about the magic angle, with correlation times ranging from 10^{-10} s for lipids (*39*) to 10^{-5} s for some large proteins such as rhodopsin (*69*), which could enhance the MAS averaging process and so produce further resolution improvement. This is in some way a two-dimensional anisotropic equivalent to liquid-state NMR where molecular motions are essential for obtaining sufficient resolution. The suppression of slow collective motions (10^{-3}–10^{-6} s) in oriented membranes is of additional help, since it has been shown to be one reason for unexpected low resolution in high-speed MAS experiments. Especially these two last points offer the opportunity to obtain proton NMR spectra from peptides and protein fragments with sufficient resolution in order to start structural studies.

This method could also be used to solve the recoupling problem which occurs in high-speed MAS studies (*18*–*22*). The spinning rate needed to obtain a well-resolved spectrum of a low-γ nucleus (^{13}C or ^{15}N) from an oriented lipid membrane might be small compared to those which would be necessary to induce the dipolar couplings to vanish, and could be of advantage for recoupling problems in structural studies of immobilized membrane components.

In order to use all of these advantages at a full scale, some technical improvements must be made. For example, using thinner glass disks would allow positioning the entire sample volume in the middle of the rotor to achieve better shimming properties and higher B_1 homogeneity. Combinations with homonuclear decoupling techniques can also be expected to contribute to an increase in spectral resolution. These studies are currently under way and will be reported later. It should be also emphasized that the possibility of studying orientations in membranes by MAOSS uses basic properties of spinning sidebands and could be the starting point of a wide range of applications.

ACKNOWLEDGMENTS

Drs. Gerhard Gröbner and Paul Spooner are acknowledged for valuable discussions and M. H. Levitt is acknowledged for providing his cc2 software.

REFERENCES

1. S. J. Opella, NMR and membrane proteins, *Nature Struct. Biol.* **4,** 845–848 (1997).
2. T. A. Cross and S. J. Opella, Solid-state NMR structural studies of peptides and proteins in membranes, *Curr. Opinion Struct. Biol.* **4,** 574–581 (1994).
3. S. O. Smith and M. Groesbeek, Magic angle spinning NMR spectroscopy of membrane proteins, *Q. Rev. Biophys.* **29,** 395–449 (1996).
4. F. M. Marassi, A. Ramamoorthy, and S. J. Opella, Complete resolution of the solid-state NMR spectrum of a uniformly ^{15}N-labeled membrane protein in phospholipid bilayers, *Proc. Natl. Acad. Sci. USA* **94,** 8551–8556 (1997).
5. X. Feng, P. J. E. Verdegem, Y. K. Lee, D. Sandstrom, M. Eden, P. BoveeGeurts, W. J. deGrip, J. Lugtenburg, H. J. M. de Groot, and M. H. Levitt, Direct determination of a molecular torsional angle in the membrane protein rhodopsin by solid-state NMR, *J. Am. Chem. Soc.* **119,** 6853–6857 (1997).
6. D. A. Middleton, R. Robins, X. L. Feng, M. H. Levitt, I. D. Spiers, C. H. Schwalbe, D. G. Reid, and A. Watts, The conformation of an inhibitor bound to gastric proton pump, *FEBS Lett.* **410,** 269–274 (1997).
7. R. Tycko, Prospects for resonance assignments in multidimensional solid-state NMR-spectra of uniformly labelled proteins, *J. Biomol. NMR* **8,** 239–251 (1996).
8. M. Mehring, ''Principles of High Resolution NMR in Solids,'' Springer-Verlag, Berlin (1983).
9. E. Oldfield, J. L. Bowers, and J. Forbes, High-resolution proton and ^{13}C NMR of membranes—Why sonicate, *Biochemistry* **26,** 6919–6923 (1987).
10. J. Forbes, C. Husted, and E. Oldfield, High-field, high-resolution proton magic-angle sample-spinning nuclear magnetic-resonance spectroscopy studies of gel and liquid-crystalline lipid bilayers and

the effects of cholesterol, *J. Am. Chem. Soc.* **110,** 1059–1065 (1988).

11. J. Forbes, J. Bowers, X. Shan, L. Moran, E. Oldfield, and M. A. Moscarello, Some new developments in solid-state nuclear magnetic-resonance spectroscopic studies of lipids and biological-membranes, including the effects of cholesterol in model and natural systems, *J. Chem. Soc. Faraday Trans.* **84,** 3821–3849 (1988).
12. J. H. Davis, M. Auger, and R. S. Hodges, High resolution ^{1}H nuclear magnetic resonance of a transmembrane peptide, *Biophys. J.* **69,** 1917–1932 (1995).
13. C. Le Guerneve and M. Seigneure, High-resolution monodimensional and multidimensional magic-angle-spinning ^{1}H nuclear-magnetic-resonance of membrane peptides in nondeuterated lipid-membranes and H_2O, *Biophys. J.* **71,** 2633–2644 (1996).
14. F. Volke and A. Pampel, Membrane hydration and structure on a subnanometer scale as seen by high-resolution solid-state nuclear-magnetic-resonance—POPC and POPC/$C_{12}EO_4$ model membranes, *Biophys. J.* **68,** 1960–1965 (1995).
15. A. Pampel and F. Volke, Rotational side bands in two-dimensional proton high-resolution MAS NMR spectra, *J. Magn. Reson. Anal.,* **3,** 222 (1997).
16. F. Volke, A. Pampel, M. Haensler, and G. Ullmann, Proton MAS NMR of a protein in a frozen aqueous-solution, *Chem. Phys. Lett.* **262,** 374–378 (1996).
17. M. Bouchard, J. H. Davis, and M. Auger, High-speed magic-angle-spinning solid-state ^{1}H nuclear-magnetic-resonance study of the conformation of gramicidin a in lipid bilayers, *Biophys. J.* **69,** 1933–1938 (1995).
18. M. H. Levitt, D. P. Raleigh, F. Creuzet, and R. G. Griffin, Theory and simulations of homonuclear spin pair systems in rotating solids, *J. Chem. Phys.* **92,** 6347–6364 (1990).
19. R. Tycko and G. Dabbagh, Measurements of S–S dipole couplings in MAS NMR (DRAMA), *Chem. Phys. Lett.* **173,** 461 (1990).
20. T. Gullion and J. Schaefer, Detection of weak heteronuclear couplings by REDOR, *Adv. Magn. Reson.* **13,** 57 (1989).
21. B. Q. Sun, P. R. Costa, D. Kocisko, P. T. Lansbury, and R. G. Griffin, Internuclear distance measurements in solid-state nuclear-magnetic-resonance—dipolar recoupling via rotor synchronized spin locking, *J. Chem. Phys.* **102,** 702–707 (1995).
22. Y. K. Lee, N. D. Kurur, M. Helmle, O. G. Johannessen, N. C. Nielsen, and M. H. Levitt, Efficient dipolar recoupling in the NMR of rotating solids—A sevenfold symmetrical radiofrequency pulse sequence, *Chem. Phys. Lett.* **242,** 304–309 (1995).
23. M. M. Maricq and J. S. Waugh, NMR in rotating solids, *J. Chem. Phys.* **70,** 3300–3316 (1979).
24. J. Herzfeld and A. E. Berger, Sideband intensities in NMR spectra, *J. Chem. Phys.* **73,** 6021 (1980).
25. H. J. M. de Groot, S. O. Smith, A. C. Kolbert, J. M. L. Courtin, C. Winkel, J. Lugtenburg, J. Herzfeld, and R. G. Griffin, Iterative fitting of magic-angle-spinning NMR spectra, *J. Magn. Reson.* **91,** 30–38 (1991).
26. K. Schmidt-Rohr and H. W. Spiess, ''Multidimensional Solid-State NMR and Polymers,'' Academic Press, London (1994).
27. Z. Y. Song, O. N. Antzutkin, Y. K. Lee, S. C. Shekar, A. Rupprecht, and M. H. Levitt, Conformational transitions of the phosphodiester backbone in native DNA: Two-dimensional magic-angle-spinning ^{31}P NMR of DNA fibers, *Biophys. J.* **73,** 1539–1552 (1997).
28. G. Gröbner, A. Taylor, P. T. F. Williamson, G. Choi, C. Glaubitz, J. A. Watts, W. J. de Grip, and A. Watts, Macroscopic orientation of natural and model membranes for structural studies, *Anal. Biochem.* **254,** 132–138 (1997).
29. J. C. Sanders, P. I. Haris, D. Chapman, C. Otto, and M. A. Heminga, Secondary structure of M13 coat protein in phospholipids studied by circular-dichroism, RAMAN, and Fourier-transform IR, *Biochemistry* **32,** 12446–12454 (1993).
30. G. Cevc and D. Marsh, ''Phospholipid Bilayers: Physical Principles and Models,'' Wiley, New York (1987).
31. M. H. Levitt, personal communication.
32. R. Smith, F. Separovic, F. C. Bennet, and B. A. Cornell, Melittin-induced changes in lipid multilayers—A solid state NMR study, *Biophys. J.* **63,** 469–474 (1992).
33. D. A. Varshalovich, A. N. Moskalev, and V. K. Khersonskii, ''Quantum Theory of Angular Momentum,'' World Scientific, Singapore (1988).
34. J. Davis, The description of membrane lipid conformation, order and dynamics by deuterium NMR, *BBA* **597,** 477–491 (1980).
35. J. Seelig, Deuterium magnetic resonance: Theory and application to lipid membranes, *Q. Rev. Biophys.* **10,** 345–418 (1977).
36. U. Haeberlen, High resolution in solids: Selective averaging, *in* ''Advances in Magnetic Resonance,'' Supplement 1, Academic Press, New York (1976).
37. U. Haeberlen, U. Kohlschütter, J. Kempf, H. W. Spiess, and H. Zimmermann, *Chem. Phys.* **3,** 248 (1974).
38. A. Watts, ''Dynamic Properties of Biomolecular Assemblies'' (S. Harding and A. J. Rowe, Eds.), pp. 320–347, Royal Chem. Soc., London (1988).
39. K. Weisz, G. Gröbner, C. Mayer, J. Stohrer, and G. Kothe, Deuteron nuclear magnetic resonance study for the dynamic organization of phospholipid/cholesterol bilayer membranes: Molecular properties and viscoelastic behavior, *Biochemistry* **31,** 1100–1112 (1992).
40. J. Stohrer, G. Gröbner, D. Reimer, K. Weisz, C. Mayer, and G. Kothe, Collective lipid motions in bilayer-membranes studied by transverse deuteron spin relaxation, *J. Chem. Phys.* **95,** 672–678 (1991).
41. M. Bloom and E. Evans, Observations of surface undulations on the mesoscopic length scale by NMR, *in* ''Biologically Inspired Physics'' (L. Pellti, Ed.), Plenum Press, New York (1991).
42. U. Haeberlen and J. S. Waugh, Coherent averaging effects in magnetic resonance, *Phys. Rev.* **175,** 453–467 (1968).
43. R. S. Prosser, S. I. Daleman, and J. H. Davis, The structure of an integral membrane peptide: A deuterium NMR relaxation study of gramicidin, *Biophys. J.* **66,** 1415–1428 (1994).
44. R. S. Prosser and J. H. Davis, Dynamics of an integral membrane peptide: A deuterium NMR relaxation study of gramicidin, *Biophys. J.* **66,** 1429–1440 (1994).
45. B. J. van Rossum, H. Forster, and H. J. de Groot, High-field and high-speed CP-MAS ^{13}C NMR heteronuclear dipolar-correlation spectroscopy of solids with frequency-switched Lee–Goldburg homonuclear decoupling, *J. Magn. Reson.* **124,** 516–519 (1997).
46. A. Sodickson and D. G. Cory, Shimming a high-resolution MAS probe, *J. Magn. Reson.* **128,** 87–91 (1997).
47. J. D. J. O'Neil and B. D. Sykes, Structure and dynamics of a detergent-solubilized membrane protein: Measurements of amide hydrogen exchange rates in M13 coat protein by ^{1}H NMR spectroscopy, *Biochemistry* **27,** 2753–2762 (1988).
48. G. D. Henry and B. D. Sykes, Assignment of amide ^{1}H and ^{15}N NMR resonances in detergent-solubilized M13 coat protein: A model for the coat protein dimer, *Biochemistry* **31,** 5284–5297 (1992).
49. F. J. M. van de Ven, J. W. M. van Os, J. M. A. Aelen, S. S. Wymenga, M. L. Remerowski, R. N. H. Konings, and C. W. Hilbers, Assignment of ^{1}H, ^{15}N, and backbone ^{13}C resonances in detergent-solubilized M13 coat protein via multinuclear multidimensional NMR—A model for the coat protein monomer, *Biochemistry* **32,** 8322–8328 (1993).

50. W. F. Wolkers, R. B. Spruijt, A. Kaan, R. N. H. Konings, and M. A. Hemminga, Conventional and saturation-transfer EPR of spin-labeled mutant bacteriophage M13 coat protein in phospholipid bilayers, *BBA—Biomembr.* **1327,** 5–16 (1997).

51. T. A. Cross and S. J. Opella, ^{1}H and ^{13}C nuclear magnetic resonance of the aromatic residues of fd coat protein, *Biochemistry* **20,** 290–297 (1981).

52. P. A. McDonnell, L. Shon, Y. Kim, and S. J. Opella, fd coat protein-structure in membrane environments, *J. Mol. Biol.* **233,** 447–463 (1993).

53. F. C. L. Almeida and S. J. Opella, fd coat protein structure in membrane environments: Structural dynamics of the loop between the hydrophobic trans-membrane helix and the amphipathic in-plane helix, *J. Mol. Biol.* **270,** 481–495 (1997).

54. G. C. Leo, L. A. Colnago, K. G. Valentine, and S. J. Opella, Dynamics of fd-coat protein in lipid bilayers, *Biochemistry* **26,** 854–862 (1987).

55. K. P. Datema, B. J. H. van Boxtel, and M. A. Hemminga, Dynamic properties of M13 coat protein in mixed bilayers. A deuterium NMR study of exchangeable sites, *J. Magn. Reson.* **77,** 372–376 (1988).

56. G. D. Henry, J. H. Weiner, and B. D. Sykes, Backbone dynamics of a model membrane-protein—^{13}C NMR-spectroscopy of alanine methyl-groups in detergent-solubilized M13 coat protein, *Biochemistry* **25,** 590–598 (1986).

57. H. D. Dettman, J. H. Weiner, and B. D. Sykes, Phenylalanyl and tyrosyl side-chain mobility in the M13 coat protein reconstituted in phospholipid-vesicles, *Biochemistry* **23,** 705–712 (1984).

58. M. J. Janiak, D. M. Small, and G. G. Shipley, Nature of the thermal pretransition of synthetic phospholipids: Dimyristoyl- and dipalmitoyl-lecithin, *Biochemistry* **15,** 4575–4577 (1976).

59. A. Watts, K. Harlos, W. Maschke, and D. Marsh, Control of structure and fluidity of phosphatidylglycerol bilayers by pH-titration, *Biochim. Biophys. Acta* **510,** 63–74 (1978).

60. C. Le Guerneve and M. Auger, New approach to study fast and slow motions in lipid bilayers—Application to dimyristoylphosphatidylcholine–cholesterol interactions, *Biophys. J.* **68,** 1952–1959 (1995).

61. B. Bechinger, L. M. Gierasch, M. Montal, M. Zasloff, and S. J. Opella, Orientations of helical peptides in membrane bilayers by solid state NMR spectroscopy, *Solid State NMR* **7,** 185–191 (1996).

62. O. N. Antzutkin, S. C. Shekar, and M. H. Levitt, Two-dimensional sideband separation in magic-angle-spinning NMR, *J. Magn. Reson. A* **115,** 7–19 (1995).

63. Z. Y. Song, O. N. Antzutkin, A. Rupprecht, and M. H. Levitt, Order-resolved side-band separation in magic-angle-spinning NMR—^{31}P NMR of oriented DNA Fibers, *Chem. Phys. Lett.* **253,** 349–354 (1996).

64. D. L. VanderHart, Characterization of the methylene ^{13}C chemical shift tensor in the normal alkane n-$C_{20}H_{42}$, *J. Chem. Phys.* **64,** 830–834 (1976).

65. K. Schmidt-Rohr, M. Wilhelm, A. Johansson, and H. W. Spiess, Determination of chemical-shift tensor orientations in methylene groups by separated-local-field NMR, *Magn. Reson. Chem.* **31,** 352–356 (1993).

66. M. Hong, J. D. Gross, and R. G. Griffin, Site-resolved determination of peptide torsion angle phi from the relative orientations of backbone N–H and C–H bonds by solid-state NMR, *J. Phys. Chem. B* **101,** 5869–5874 (1997).

67. X. Feng, Y. K. Lee, D. Sandstrom, M. Eden, H. Maisel, A. Sebald, and M. H. Levitt, Direct determination of a molecular torsional angle by solid-state NMR, *Chem. Phys. Lett.* **257,** 314–320 (1996).

68. Y. Tomita, E. J. O'Connor, and A. McDermott, A method for dihedral angle measurement in solids—Rotational resonance NMR of a transition-state inhibitor of triose phosphate isomerase, *J. Am. Chem. Soc.* **116,** 8766–8771 (1994).

69. N. J. P. Ryba and D. Marsh, Protein rotational diffusion and lipid protein interactions in recombinants of bovine rhodopsin with saturated diacylphosphatidylcholines—Different chain lengths studied by conventional and saturation-transfer electron-spin-resonance, *Biochemistry* **31,** 7511–7518 (1992).